Liquid Crystals

International Edition: DOI: 10.1002/anie.201410662
German Edition: DOI: 10.1002/ange.201410662

A Perfect Match: Fullerene Guests in Star-Shaped Oligophenylenevinylene Mesogens**

Matthias Lehmann and Markus Hügel*

Dedicated to Professor Herbert Meier on the occasion of his 75th birthday

Abstract: *Star-shaped oligophenylenevinylene (OPV) mesogens are shape-persistent and possess formally large void space. A mesogen with three styrene repeating units packs densely in a columnar helical arrangement. Attachment of one fullerene through a short spacer results in an exceptional increase of the mesophase stability. X-ray scattering and modeling evidence a triple-helical arrangement in which the fullerene perfectly fills the void space between the arms of the star mesogen.*

In all kinds of materials, the control of morphology is decisive for their mechanical or electronic performance. Nature is a perfect example in this respect, where the position of functional units is precisely controlled by self-assembly processes, for example, in the photosynthetic apparatus, enzymes, or transport proteins. Also in artificial materials a high degree of complexity and its control has been achieved. Some recent examples are complex liquid-crystalline (LC) materials forming polygonal cylinder phases,[1] shape-persistent macrocycles with void space along the columns,[2] or LCs containing nanoparticles, such as fullerene,[3,4] or magnetic clusters.[5] Earlier studies investigated the self-assembly of fullerene–oligophenylenevinylene dimers in lamellar and columnar structures and their photophysical properties.[6,7] Fullerene–phthalocyanine[8] or fullerene–porphyrine dyads[9] with laterally attached fullerenes have recently been shown to aggregate in highly ordered columnar structures which may be of interest for photovoltaic applications.

Herein we combine non-conventional oligophenylenevinylene star-mesogens, known to stack in columnar phases,[10] with fullerene C_{60} attached in the center of the star by a short spacer. The self-assembly process of these non-conventional mesogens is essentially based on nanosegregation of their core scaffold from the peripheral aliphatic chains and the optimization of space-filling. In contrast to semi-flexible star-mesogens for which the packing can be optimized by folding the molecules to *E*-shaped or cone-shaped conformers,[11] the shape-persistent OPV stars maintain their overall star-morphology and exhibit large void space between their arms. Herein we highlight the unique self-assembly of OPV-star **1** and star-OPV-fullerene hybrids **2c**, in which the void is perfectly filled by non-mesomorphic fullerene guests (Figure 1). These guests facilitate the space filling and stacking in columnar structures and consequently increase the mesophase stability by more than 70 °C compared to the parent mesogen **1**.

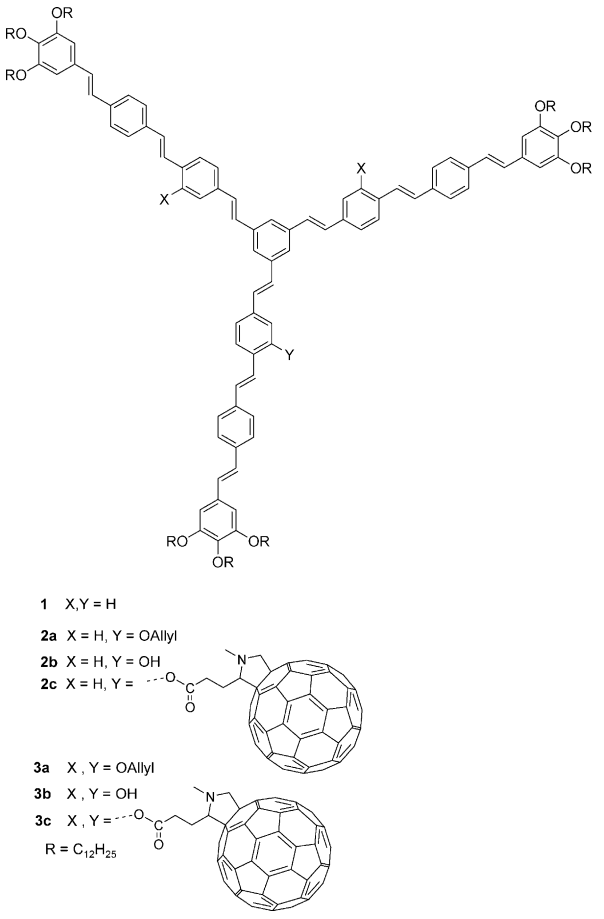

Figure 1. OPV stars and fullerene–OPV hybrid stars.

The synthesis of the target OPV–fullerene hybrids has to be planned carefully, especially for derivatives with three fullerenes attached to one star. A fully convergent route, in which the fullerene–OPV arm undergoes a threefold Wittig–Horner coupling in the final step, as used for many stilbenoid dendrimers,[10] is not compatible with fullerene chemistry

[*] Prof. Dr. M. Lehmann, M. Hügel
Institute of Organic Chemistry
University of Würzburg
Am Hubland, 97074 Würzburg (Germany)
E-mail: Matthias.Lehmann@uni-wuerzburg.de

[**] We are grateful to Prof. H. Detert (University of Mainz) for elemental analysis and to the DFG for financial support.

Supporting information for this article is available on the WWW under http://dx.doi.org/10.1002/anie.201410662.

since the nucleophile will not only attack the aldehyde but also the fullerene derivative.[12] The coupling of fullerene by a Prato reaction in the final step,[13] after a convergent synthesis of the stilbenoid star with spacer to avoid protecting-group chemistry, has been discarded, since several couplings with the same fullerene may result. Therefore, we decided to follow a tried-and-tested strategy.[6c] First the stilbenoid scaffold was prepared by a convergent route using the allyl group to protect the point of spacer connection; subsequently the protecting group was cleaved and the fullerene with spacer was attached by an esterification reaction. Scheme 1 summarizes the synthesis of the target compounds **1**–**3**. The key intermediate is arm **6**, which was obtained by the coupling of phosphonate **4** with aldehyde **5** in a good over all yield of 68%. This protected arm was then converted into non-C_3-symmetric **2a** with phosphonate **8** and into star **3a** by threefold coupling with trisphosphonate **10**. The protecting groups had to be carefully cleaved and the final esterification reaction with fullerene derivative **11**[14] afforded the target compounds **2c** and **3c**. The last step appeared to be challenging with yields between 52–64% per esterification step. The parent star without fullerene was obtained by a threefold Wittig–Horner reaction of trisaldehyde **9**[15] with phosphonate **4**. The identity and purity of all the target compounds are demonstrated by standard analytical methods (see Supporting Information).

The thermotropic properties of the star-shaped compounds **1**, **2c**, **3c** and the mixture **M3** (**1**:**3c** = 2:1) were studied by polarized optical microscopy (POM), differential scanning calorimetry (DSC), and X-ray scattering (Table 1). All materials, except **3c**, self-assemble in liquid-crystalline phases with broad temperature ranges and transform at low temperature to LC glasses. Pseudo-focal conic textures point to columnar phases and X-ray scattering evidences hexagonal symmetry (see Figure 2, Figure 3 and Supporting Information). It has to be stressed that the stability of the mesophase increases by more than 70°C upon attachment of one fullerene in **2c**. Fullerene is a spherical building block and has, among others, been incorporated in LC phases by coupling to mesogenic dendrons of various generations.[16] Nanosegregation of the different building blocks has been proposed as a self-assembly mechanism. In all cases, independent of the liquid-crystal structure, the clearing temperatures, and thus the mesophase stabilities decreased compared to the fullerene free materials. Consequently, the enormous increase in the clearing temperature of the star-mesogen **2c** and mixture **M3** compared to compound **1** shows that not only nanosegregation but other factors improve the packing and consequently the intermolecular interactions in the columnar phase.

To understand this surprising behavior, the packing of parent star-mesogen **1** was investigated by wide-, middle-, and small-angle X-ray scattering (WAXS, MAXS, and SAXS) and modelled using Materials Studio (Force field Compass). Figure 2 shows the 2D X-ray pattern at 25°C obtained using an extruded fiber for which the columns are

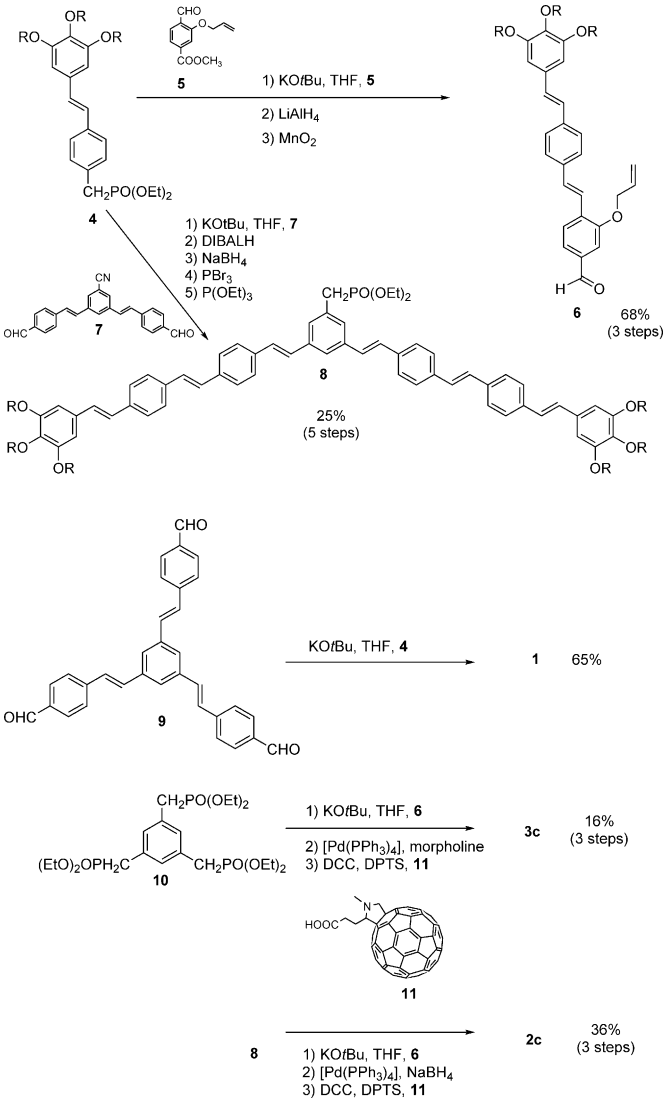

Scheme 1. Synthesis of the target structures. DCC = Dicyclohexylcarbodiimide, DIBALH = Diisobutylaluminiumhydrid, DPTS = 4-(Dimetylamino)pyridinium 4-toluenesulfonate.

Table 1: Thermotropic properties and X-ray data of star-mesogens.

Compound	Transition temp. (onset) [°C]/ΔH [kJ mol^{-1}][a]	*a* [Å] (T/°C)	*c* [Å][b]	δ_{Xray} (δ_{exp}) [g cm^{-3}][c]
1	Col_h 205.5/2.4 I	61.5 (25)	43.6	0.99 (0.98)
2c	Col_h 280.5/2.9 I	56.1 (25)	102.6	1.00 (>0.99)
3c	Cr > 300 decomp.	–	–	
M3 (**1**:**3c** = 2:1)	Col_h 275 I[d]	56.0 (30)	101.7	1.01 (–)

[a] All compounds decompose slowly when kept in their isotropic liquid for a prolonged time Col_h = columnar hexagonal LC phase, Cr = crystalline phase, I = isotropic liquid. [b] *c* parameter calculated based on the meridional diffuse signals. [c] X-ray density calculated with *N* = 32 (**1**) and *N* = 48 (**2c**, **3c**) molecules in the unit cell at room temperature. The experimental values at 22°C were obtained by the buoyancy method using water/methanol mixtures (for details see Supporting Information). [d] Clearing temperature observed in POM and as peak of DSC (broad signal); the onset temperature is 254°C.

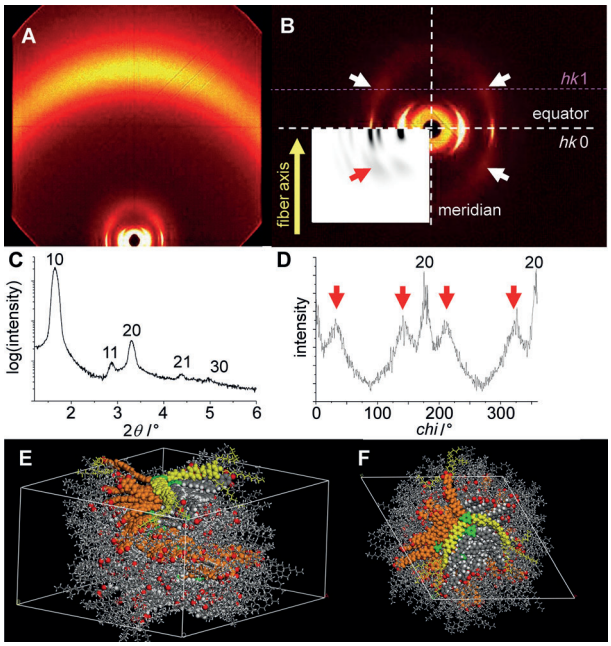

Figure 2. Stilbene star mesogen **1**. X-ray diffraction pattern A) WAXS, B) MAXS. Inset: X-ray diffraction simulation. C) Integrated intensity along the equator of the diffraction pattern showing the reflections indexed according to the hexagonal symmetry. Chi scan between $2\theta = 3.3$–$4.0°$ showing the intensity of the diffuse set of four meridional signals. D) The peaks at approximately 0° and 180° correspond to the 20 reflection. Modeling of the columnar phase—helical packing with short correlation length highlighted for one arm (orange); center of mesogens (green), one complete molecule (additional arms in yellow); side view (E), top view (F).

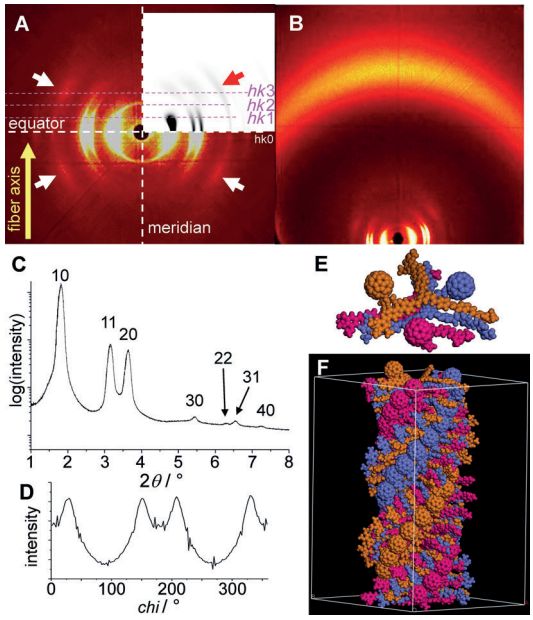

Figure 3. Star-mesogen **2c**. A) X-ray diffraction pattern (MAXS) at 25 °C with X-ray simulation based on the triple helical packing of the core. B) WAXS pattern at 25 °C. C) Integration of the pattern along the equator (theta scan) and D) chi-scan between $2\theta = 4.6$–$5.8°$. E) Aggregate of three mesogens omitting the CH_2 groups for clarity. F) Model of the triple-helical stacking of the core building block.

oriented along the fiber axis. In addition to the principle reflections at the equator (hk0) indicating the hexagonal symmetry, a halo corresponds to an average distance of 4.6 Å. Further intensities related to a π–π distance are not observed. However, four diffuse signals, left and right of the meridian in the small-angle region of the pattern, clearly indicate a correlation along the column direction (Figure 2B,D). Assuming that the diffuse signals are positioned at the *hk*1 layer line, the *c* parameter is deduced to be 43.6 Å. If the molecules co-facially stack with a typically small π–π distance of, for example, 3.4 Å, then only 13 mesogens (43.6 Å/3.4 Å) could assemble in the column, resulting in a density of less than 0.40 g cm^{-3}. The minimum value for the density at 22 °C has been experimentally obtained to be 0.98 g cm^{-3} (Table 1), thus the cell must contain at least 32 molecules and co-planar stacking is not feasible. Since the packing of star mesogens can be optimized by helical self-assembly,[17] it is reasonable to assume a helical packing also occurs here. Modeling of the phase at a density of 0.99 g cm^{-3}, that is, 32 mesogens in the unit cell (for details see Supporting Information), reveals, that the packing and nanosegregation of aromatic and aliphatic parts of this large number of molecules is possible by helical assembly and lateral translational displacement of the molecular centers from the columnar axis to avoid steric repulsion along the stacking direction (Figure 2E,F). Further, it is evident that the stilbenoid scaffold is conformationally deformed from the idealistic planar C_3-symmetric structure leading to an increase of torsional energy. However, this increase is much less than the gain in attractive intermolecular, non-bonding interaction (electrostatic and van der Waals interaction, see Supporting Information), presumably because the anharmonic potential curve for rotation of the benzene rings out of the plane of the double bond is very flat.[18] The correlation of the helical assembly within the hexagonal phase, estimated from the half-width at half maximum, is low and amounts approximately to only 4–5 repeating units (helical pitches).[19] The inset of the X-ray pattern shows a simulated X-ray pattern for a fiber and is in good agreement with the experimental data.

The high mesophase stability of star compound **2c** indicates that the fullerene increases the intermolecular interaction and the order in the system. Indeed X-ray diffraction reveals three unusual strong reflections at small angles indicating a rather high order of the columnar phase (Figure 3A–C). Again, a set of diffuse signals at the meridian shows a correlation along the column axis ($d = 34.2$ Å) indicating a helical arrangement. The correlation length increases by a factor of two (10 repeating units) compared to star **1**. Apparently the fullerene attached by the short spacer must fill one of the three cavities of the stilbenoid star. In an aggregate of three mesogens, the fullerenes occupy all three cavities (Figure 3E; orange, red, and blue molecules). An optimal dense packing of the fullerenes along the column is achieved by helical stacking. The helical pitch of **2c** is 102.6 Å which is three times the *d* value and contains 48 mesogens. The distance of the planes normal to the axis of the helix, in which the molecular building blocks are positioned on average, amounts to 2.14 Å (102.60 Å/48) for the stilbenoid scaffold and 6.42 Å for the fullerenes. Thus,

fullerenes with a diameter of approximately 10 Å must interdigitate along the column as shown in Figure 3F. Owing to the space-filling by the fullerene, the distance between the planes normal to the axis of the helix along the column is greater than for star **1** (43.60 Å/32 = 1.36 Å). Since the single molecules (**1**, **2c**) are decorated on the periphery with the same number, that is, with nine dodecyloxy chains, an arbitrary columnar unit of 10 Å length contains 66 dodecyloxy chains in the case of compound **1** and only 42 chains for compound **2c**. Therefore, the hexagonal parameter *a* for the fullerene derivative **2c** decreases by more than 5 Å compared to compound **1** (Table 1).

Modeling and simulation of the X-ray pattern of the phase, in which the reflections of the first two layer lines are extinct, point to a triple helix. The simulation pattern of such a triple helix of the mesogen cores is in a good agreement with the experimental data (Figure 3A (inset)). Thus fullerene guests occupy the cavities of such star mesogens. They segregate in their own compartments and optimize their intermolecular interaction by a dense helical packing. This model is further supported by the fact that mixture **M3** (star **1**:star **3c** = 2:1), in which star **3c** contains a fullerene at each arm, forms a mesophase with a stability similar to that of neat compound **2c** with a clearing temperature at 275 °C (POM). Note that the neat compound **3c** is not liquid crystalline—it melts at temperatures above 300 °C under decomposition. The X-ray experiments of the mixture give almost identical cell parameters to star **2c** (Table 1). Thus a similar model for the mixture can be envisaged in which the fullerenes fill the void in the three cavities. Along the columns one molecule **3c** is flanked by two stars **1** which results in an assembly which is very much related to the model of the trimer of compound **2c**. The lower order revealed by the more-diffuse and less-intense X-ray signals along the meridian indicate that the ideal stacking **1**/**3c**/**1** is not perfectly realized, because of either an imperfect mixture or natural occurring defects (see Supporting Information).

The photophysical properties of **1**, **2c**, **3c** in solution and **1**, **2c** in thin solid films have been studied by UV/Vis- and fluorescence spectroscopy (Figure 4). All compounds show an absorption maximum in $CHCl_3$ at 400 nm and the fullerene derivatives have additional absorption maxima at 255 nm, 327 nm, and a shoulder at 470 nm (Figure 4, arrow). With the increasing fullerene content these fullerene features increase as expected for compound **3c**. The fluorescence spectrum shows a strong emission at 468 nm of the stilbenoid star, which is efficiently quenched to only 10% of that of star **1** when fullerene is attached in **2c**. The emission is even more efficiently extinguished in compound **3c** with three fullerenes because all the OPV units always have a fullerene in their vicinity. In contrast to the fluorescence spectra in solution, the emission is quantitatively quenched in the solid state, which is naturally explained by the packing of the fullerene triple helix. In the solid state the OPV arms are always side by side to fullerene aggregates, thus an effective charge transfer may occur.[6b,c] These results are promising with respect to a possible application in organic photovoltaic materials.

In summary, a fullerene attached by a short spacer to a star-shaped mesogen as in compound **2c** enormously

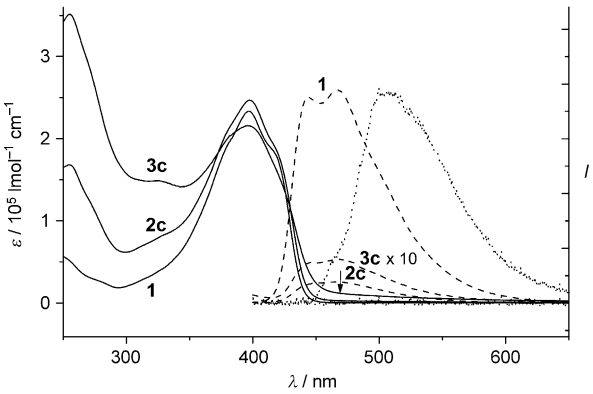

Figure 4. Absorption spectra (solid lines) from bottom to top: compound **1**, **2c**, and **3c** in $CHCl_3$. Emission spectra (dashed lines) from bottom to top: compound **2c**, **3c** (magnified by a factor of 10) and **1** in $CHCl_3$, and emission of thin solid films (dotted lines) of **1** and **2c** (no intensity). The arrow indicates the shoulder at 470 nm in the absorption of **3c**. For colored version see Supporting Information.

increases the mesophase stability compared to the parent stilbenoid star **1**. The neat star **1** assembles in a dense helical arrangement with 32 mesogens placed along 43.6 Å by rotational and positional displaced molecules from the center of the column and conformational deformations to avoid steric crowding and optimize space filling. In the hybrid derivative **2c** and the mixture between **3c** and **1**, fullerene fills a great portion of the void space between the arms and facilitates the columnar stacking. The systems optimize the packing of fullerenes by the arrangement in a triple helix. Such highly ordered, columnar donor (stilbenoid scaffold)–acceptor (fullerene) assemblies are interesting materials for organic electronics and especially photovoltaic applications if they can be oriented at surfaces. Therefore, synthetic work is in progress to lower the clearing temperatures of these hybrid materials to produce liquid-crystal cells with highly oriented material using alignment layers.

Keywords: columnar phases · donor–acceptor systems · fullerenes · helical packing · liquid crystals

How to cite: *Angew. Chem. Int. Ed.* **2015**, *54*, 4110–4114
Angew. Chem. **2015**, *127*, 4183–4187

[1] C. Tschierske, *Angew. Chem. Int. Ed.* **2013**, *52*, 8828–8878; *Angew. Chem.* **2013**, *125*, 8992–9047.
[2] M. Fritzsche, A. Bohle, D. Dudenko, U. Baumeister, D. Sebastiani, G. Richardt, H. W. Spiess, M. R. Hansen, S. Höger, *Angew. Chem. Int. Ed.* **2011**, *50*, 3030–3033; *Angew. Chem.* **2011**, *123*, 3086–3089.
[3] D. Felder-Flesch, D. Guillon, B. Donnio, in *Handbook of Liquid Crystals*, *Vol. 5* (Eds.: J. W. Goodby, P. J. Collings, T. Kato, C. Tschierske, H. F. Gleeson, P. Raynes), Wiley-VCH, Weinheim, **2014**, pp. 317–361.
[4] K. Toth, J. K. Molloy, M. Matta, B. Heinrich, D. Guillon, G. Bergamini, F. Zerbetto, B. Donnio, P. Ceroni, D. Felder-Flesch, *Angew. Chem. Int. Ed.* **2013**, *52*, 12303–12307; *Angew. Chem.* **2013**, *125*, 12529–12533.
[5] E. Terazzi, G. Rogez, J.-L. Gallani, B. Donnio, *J. Am. Chem. Soc.* **2013**, *135*, 2708–2722.

[6] a) S. Campidelli, R. Deschenaux, J.-F. Eckert, D. Guillon, J.-F. Nierengarten, *Chem. Commun.* **2002**, 656 – 657; b) A. Gégout, J.-F. Nierengarten, B. Delavaux-Nicot, C. Duhayon, A. Saquet, A. Listorti, A. Belbakra, C. Chiorboli, N. Armaroli, *Chem. Eur. J.* **2009**, *15*, 8825 – 8833; c) A. Gégout, M. Holler, T. M. Figueira-Duarte, J.-F. Nierengarten, *Eur. J. Org. Chem.* **2008**, 3627 – 3634.
[7] T. Nhu Y. Hoang, D. Pociecha, M. Salamonczyk, E. Gorecka, R. Deschenaux, *Soft Matter* **2011**, *7*, 4948 – 4953.
[8] H. Hayashi, W. Nihashi, T. Umeyama, Y. Matano, S. Seki, Y. Shimizu, H. Imahori, *J. Am. Chem. Soc.* **2011**, *133*, 10736 – 10739.
[9] C.-L. Wang, W.-B. Zhang, R. M. Van Horn, Y. Tu, X. Gong, S. Z. D. Cheng, Y. Sun, M. Tong, J. Seo, B. B. Y. Hsu, A. J. Heeger, *Adv. Mater.* **2011**, *23*, 2951 – 2956.
[10] M. Lehmann, B. Schartel, M. Hennecke, H. Meier, *Tetrahedron* **1999**, *55*, 13377 – 13394.
[11] M. Lehmann, in *Handbook of Liquid Crystals*, *Vol. 5* (Eds.: J. W. Goodby, P. J. Collings, T. Kato, C. Tschierske, H. F. Gleeson, P. Raynes), Wiley-VCH, Weinheim, **2014**, pp. 243 – 315.
[12] a) A. Hirsch, M. Brettreich, *Fullerenes—Chemistry and Reactions*, Wiley-VCH, Weinheim **2005**; b) H. J. Bestmann, D. Hadawi, T. Röder, C. Moll, *Tetrahedron Lett.* **1994**, *35*, 9017 – 9020.
[13] a) M. Prato, M. Maggini, *Acc. Chem. Res.* **1998**, *31*, 519 – 526; b) M. Maggini, G. Scorrano, M. Prato, *J. Am. Chem. Soc.* **1993**, *115*, 9798 – 9799.
[14] A. Ohashi, A. Satake, Y. Kobuke, *Bull. Chem. Soc. Jpn.* **2004**, *77*, 365 – 374.
[15] E. Díez-Barra, J. C. García-Martínez, S. Merino, R. del Rey, J. Rodríguez-López, P. Sánchez-Verdú, J. Tejeda, *J. Org. Chem.* **2001**, *66*, 5664 – 5670.
[16] a) R. Deschenaux, B. Donnio, D. Guillon, *New J. Chem.* **2007**, *31*, 1064 – 1073; b) N. Maringa, J. Lenoble, B. Donnio, D. Guillon, R. Deschenaux, *J. Mater. Chem.* **2008**, *18*, 1524 – 1534.
[17] a) A. R. A. Palmans, J. A. J. M. Vekemans, H. Fischer, R. A. Hikmet, E. W. Meijer, *Chem. Eur. J.* **1997**, *3*, 300 – 307; b) C. Roche, H.-J. Sun, M. E. Prendergast, P. Leowanawat, B. E. Partridge, P. A. Heiney, F. Araoka, R. Graf, H. W. Spiess, X. Zeng, G. Ungar, V. Percec, *J. Am. Chem. Soc.* **2014**, *136*, 7169 – 7185; c) M. Lehmann, in *Handbook of Liquid Crystals*, *Vol. 5* (Eds.: J. W. Goodby, P. J. Collings, T. Kato, C. Tschierske, H. Gleeson, P. Raynes), Wiley-VCH, Weinheim, **2014**, pp. 243 – 315.
[18] H. Meier, *Angew. Chem. Int. Ed. Engl.* **1992**, *31*, 1399 – 1420; *Angew. Chem.* **1992**, *104*, 1425 – 1446.
[19] a) R. Jenkens, R. L. Snyder, *Chemical Analysis: Introduction to X-ray Powder Diffractometry*, *Vol. 138*, Wiley, New York, **1996**; b) P. Scherrer, *Nachr. Ges. Wiss. Göttingen, Math.-Phys. Kl.* **1918**, *2*, 98 – 100.

Received: November 1, 2014
Published online: February 4, 2015

